BIOORGANIC CHEMISTRY **24,** 127–149 (1996)
ARTICLE NO. 0012

7-*S*-Glutathionyltryptophan-4,5-dione: Formation from 5-Hydroxytryptophan and Reactions with Glutathione

ZHENG WU AND GLENN DRYHURST[1]

Department of Chemistry and Biochemistry, University of Oklahoma, Norman, Oklahoma 73019

Received September 8, 1995

The electrochemically driven oxidation of 5-hydroxytryptophan (5-HTPP) in the presence of free glutathione (GSH) yields 4-*S*-glutathionyl-5-hydroxytryptophan (**5**) and 7-*S*-glutathionyltryptophan-4,5-dione (**7**). The latter glutathionyl conjugate is formed both by nucleophilic addition of GSH to tryptophan-4,5-dione (**4**), a normal product of the oxidation of 5-HTPP, and by oxidation of **5** in a reaction where the glutathionyl residue migrates from the C(4)- to the C(7)-position. In the presence of free GSH **7** reacts to give the 3,7- and 6,7-bi-*S*-glutathionyl conjugates of **4** and, as a result of intramolecular cyclization reactions, a number of glutathionyl conjugates of an unusual tricyclic pyrroloquinoline. It is speculated that one or more of these products might represent aberrant oxidative metabolites that have been detected in the cerebrospinal fluid of patients with Alzheimer's Disease.

INTRODUCTION

Analysis of the cerebrospinal fluid (CSF) of Alzheimer's Disease (AD) patients has demonstrated the presence of abnormal metabolites of 5-hydroxytryptamine (5-HT) and 5-hydroxytryptophan (5-HTPP) which are not present in the CSF of age-matched controls (*1*). Although the identities of such apparently aberrant metabolites are unknown, evidence has been presented that they are oxidized forms of 5-HT and 5-HTPP (*2*). Many lines of evidence indicate that oxidative damage occurs in the AD brain. To illustrate, significantly elevated levels of oxidized proteins (*3*) and lipids (*4*) have been measured in certain regions of AD brains. In part, such oxidative damage might be mediated by increased production of oxygen radical species as evidenced by increased activities of superoxide dismutase (*5, 6*), glucose-6-phosphate dehydrogenase (*7*), and glutathione peroxidase (*8*). Oxidative damage to the brain in AD and a number of other neurodegenerative disorders is widely believed to primarily affect proteins, lipids, and DNA (*9*). However, it is of interest to note that certain serotonergic, noradrenergic, and dopaminergic pathways are severely degenerated in AD and many other degenerative brain diseases. These neuronal systems employ the neurotransmitters 5-HT, norepinephrine, and dopamine, which are very easily oxidized substances. On a chemical basis, therefore, it seems extremely unlikely that these neurotransmitters and their easily oxidizable precursors and metabolites would be spared from oxygen radical-mediated or other

[1] To whom correspondence should be addressed.

0045-2068/96 $18.00

forms of oxidation chemistry. Detection of trace levels of unknown but aberrant oxidized forms of 5-HTPP and 5-HT in the CSF of AD patients (*1, 2*) provides support for the latter conclusion. This laboratory, therefore, has been exploring the hypothesis that aberrant oxidative metabolism of 5-HTPP and 5-HT might yield abnormal metabolites that contribute to the neurodegeneration that occurs in certain regions of the brain in AD and other neurodegenerative brain disorders. Recently, we reported on the electrochemically driven and various enzyme-mediated oxidations of 5-HTPP at physiological pH (*10*). These reactions appeared to proceed by very similar *chemical* pathways to a large number of products at least one of which is an extremely toxic compound when administered into the brains of laboratory animals (*11*). However, in the event that aberrant oxidation of 5-HTPP does occur in the AD brain, such reactions are likely to occur in the cytoplasm of serotonergic nerve terminals and axons. Accordingly, electrophilic intermediates and products formed as a result of oxidation of 5-HTPP (*10*) would necessarily be exposed to a number of powerful intraneuronal nucleophiles. These would include L-cysteine (CySH) and, more importantly, glutathione (GSH) (*12, 13*). Recently, it was demonstrated that GSH and CySH can partially divert the electrochemical and enzymatic oxidation of 5-HT at physiological pH by scavenging such electrophilic intermediates and products (*14, 15*). A significant product formed in the oxidation of 5-HT in the presence of free GSH was 7-*S*-glutathionyltryptamine-4,5-dione (*14*). This putative aberrant oxidative metabolite of 5-HT is lethal when administered into the brains of mice, evokes a profound behavioral response, alters whole brain levels of several neurotransmitters/metabolites, and possesses other chemical and neuropharmacological properties that might be of relevance to the pathoetiology of AD (*16*). Initially, the goal of the work described was to investigate the influence of GSH on the oxidation chemistry of 5-HTPP at pH 7.4 and, most particularly, to isolate 7-*S*-glutathionyltryptophan-4,5-dione such that the neuropharmacological/neurotoxicological properties of this compound could be compared to the corresponding analog derived from 5-HT. However, it was discovered that in both the absence and the presence of free GSH, 7-*S*-glutathionyltryptophan-4,5-dione undergoes a number of unusual secondary reactions that are described in this communication.

EXPERIMENTAL

L-5-Hydroxytryptophan, glutathione (free base), and trifluoroacetic acid (TFA) were obtained from Sigma (St. Louis, MO). HPLC-grade acetonitrile (MeCN) was obtained from Fisher (Springfield, NJ).

Voltammograms were obtained using a pyrolytic graphite electrode (PGE; Pfizer Minerals, Pigments and Metals Division, Easton, PA) having an approximate surface area of 4 mm^2 (*17*) and a BAS-100A electrochemical analyzer (Bioanalytical Systems, West Lafayette, IN). A conventional three-electrode electrochemical cell containing a platinum gauze counter electrode and a saturated calomel reference electrode (SCE) was employed for cyclic voltammetry. All cyclic voltammograms

were corrected for iR drop. Test solutions were thoroughly deoxygenated with a vigorous stream of N_2 gas for about 5 min before voltammograms were recorded.

Controlled potential electrolyses were performed with a Brinkman Instruments (Westbury, NY) Model LT73 potentiostat and three compartment cells in which the working, counter, and reference electrode compartments were separated with a Nafion membrane (Type 117; DuPont, Wilmington, DE). One cell had a working electrode compartment capacity of 40 ml and a working electrode consisting of several plates of pyrolytic graphite having a total surface area of ca. 100 cm^2. The other cell had a working electrode compartment capacity of 350 ml and pyrolytic graphite electrodes having a total surface area of ca. 300 cm^2. The counter electrodes were platinum gauze and the reference electrode was the SCE. All potentials are referenced to the SCE at ambient temperature (22 ± 2°C).

HPLC employed two Gilson (Middleton, WI) binary gradient systems. The analytical HPLC was equipped with two Model 302 pumps (5-ml pump heads) and a Waters (Milford, MA) Model 440 UV detector set at 254 nm. The preparative HPLC was equipped with Model 305 and Model 306 pumps (25-ml pump heads) and a Gilson Holochrome UV detector (254 nm). In analytical HPLC, samples were introduced onto a reversed-phase column (Brownlee Laboratories; RP-18 packing, 5 μm, 250 × 7 mm) protected with a short guard column (Brownlee RP-18; 5 μm, ODGU, 50 × 5 mm) by means of a Rheodyne (Cotati, CA) Model 7125 injector equipped with a 2.0-ml sample loop. In preparative HPLC, some samples (1–10 ml) were introduced onto a reversed-phase column (J. T. Baker, Phillipsburg, NY; Bakerbond C_{18}, 10 μm, 250 × 21.2 mm), protected by a guard column (50 × 9 mm) packed with the same stationary phase, with a Rheodyne 7125 injector equipped with a 10-ml sample loop. Larger sample volumes (>10–100 ml) were pumped directly onto the column through one of the HPLC pumps.

A number of mobile-phase solvents were employed for HPLC and used deionized water (H_2O), concentrated ammonium hydroxide solution (NH_4OH), glacial acetic acid (HOAc), concentrated TFA, and HPLC-grade MeCN. These various mobile-phase solvents were: solvent A (10.0 ml of NH_4OH, 4 liters of H_2O, HOAc to pH 3.8), solvent B (2 liters of solvent A plus 2 liters of MeCN), solvent C (15.0 ml of NH_4OH, 4 liters of H_2O, TFA to pH 2.6), solvent D (2 liters of solvent C plus 2 liters of MeCN), solvent E (H_2O), solvent F (800 ml of H_2O plus 3200 ml of MeCN), solvent G (30 ml of NH_4OH, 4 liters of H_2O, HOAC to pH 7.0), solvent H (2 liters of solvent G plus 2 liters of MeCN), solvent I (H_2O adjusted to pH 2.8 with TFA), and solvent J (2 liters of solvent I plus 2 liters of MeCN).

The gradient profiles employed for each HPLC method were as follows: preparative method I (0–0.5 min, 100% solvent A, linear increase of flow rate from 10 to 15 ml min^{-1}; 0.5–12 min, linear increase to 12% solvent B, flow rate 15 ml min^{-1}, 12–25 min, linear increase to 20% solvent B, 15 ml min^{-1}; 25–41 min, linear increase to 75% solvent B, 15 ml min^{-1}; 41–42 min, linear increase to 100% solvent B, 15 ml min^{-1}; 42–48 min, 100% solvent B, 15 ml min^{-1}), analytical method II (0–1.0 min, 100% solvent A, linear increase from 2.0 to 3.0 ml min^{-1}; 1–2 min, 100% solvent A, 3 ml min^{-1}; 2–8 min, linear increase to 14% solvent B, 3 ml min^{-1}; 8–18 min, linear increase to 23% solvent B, 3 ml min^{-1}; 18–32 min, linear increase to 40% solvent B, 3 ml min^{-1}; 32–33 min, linear increase to 100% solvent B, 3 ml

min^{-1}; 33–39 min, 100% solvent B, 3 ml min^{-1}), preparative method III (0–0.5 min, 100% solvent G, linear increase from 10 to 15 ml min^{-1}; 0.5–10 min, linear increase to 10% solvent H, 15 ml min^{-1}; 10–28 min, linear increase to 17% solvent H, 15 ml min^{-1}; 28–29 min, linear increase to 100% solvent H, 15 ml min^{-1}; 29–40 min, 100% solvent H, 15 ml min^{-1}), preparative method IV (0–0.5 min, 100% solvent G, linear increase from 10 to 15 ml min^{-1}; 0.5–16 min, linear increase to 20% solvent H, 15 ml min^{-1}; 16–35 min, linear increase to 28% solvent H, 15 ml min^{-1}; 35–36 min, linear increase to 100% solvent H, 15 ml min^{-1}; 36–43 min, 100% solvent H, 15 ml min^{-1}), preparative method V (0–1 min, 100% solvent I, linear increase from 10 to 15 ml min^{-1}; 1–8 min, 100% solvent I, 15 ml min^{-1}; 8–20 min, linear increase to 18% solvent J, 15 ml min^{-1}; 20–40 min, linear increase to 33% solvent J, 15 ml min^{-1}; 40–41 min, linear increase to 100% solvent J, 15 ml min^{-1}; 41–45 min, 100% solvent J, 15 ml min^{-1}), preparative method VI (0–1 min, 100% solvent E, linear increase from 10 to 15 ml min^{-1}; 1–10 min, 100% solvent E, 15 ml min^{-1}; 10–20 min, linear increase to 80% solvent F, 15 ml min^{-1}; 20–24 min, linear increase to 100% solvent F, 15 ml min^{-1}; 24–26 min, 100% solvent F, 15 ml min^{-1}), analytical method VII (0–1 min, 100% solvent A, linear increase from 2 to 3 ml min^{-1}; 1–6 min, 100% solvent A, 3 ml min^{-1}; 6–10 min, linear increase to 2% solvent B, 3 ml min^{-1}; 10–22 min, linear increase to 20% solvent B, 3 ml min^{-1}; 22–32 min, linear increase to 60% solvent B, 3 ml min^{-1}; 32–33 min, linear increase to 100% solvent B, 3 ml min^{-1}; 33–37 min, 100% solvent B, 3 ml min^{-1}), preparative method VIII (0–3 min, 100% solvent A, linear increase from 10 to 15 ml min^{-1}; 3–15 min, linear increase to 7% solvent B, 15 ml min^{-1}; 15–40 min, linear increase to 70% solvent B, 15 ml min^{-1}; 40–41 min, linear increase to 100% solvent B, 15 ml min^{-1}; 41–46 min, 100% solvent B, 15 ml min^{-1}), analytical method IX (0–1 min, 100% solvent C, linear increase from 2 to 3 ml min^{-1}; 1–10 min, linear increase to 10% solvent D, 3 ml min^{-1}; 10–20 min, linear increase to 25% solvent D, 3 ml min^{-1}; 20–28 min, linear increase to 40% solvent D, 3 ml min^{-1}; 28–29 min, linear increase to 100% solvent D, 3 ml min^{-1}), preparative method X (0–1 min, 100% solvent E, linear increase from 10 to 15 ml min^{-1}; 1–10 min, 100% solvent E, 15 mL min^{-1}; 10–20 min, linear increase to 80% solvent F, 15 ml min^{-1}; 20–24 min, linear increase to 100% solvent F, 15 ml min^{-1}; 24–26 min, 100% solvent F, 15 ml min^{-1}).

Fast atom bombardment mass spectrometry (FAB–MS) was carried out with a VG Instruments (Manchester, UK) ZAB-E spectrometer. NMR spectra were recorded on a Varian (Palo Alto, CA) XL-300 spectrometer. Ultraviolet–visible spectra were recorded on a Hewlett–Packard 8452A diode array spectrophotometer.

Synthesis and Purification of Tryptophan-4,5-dione **(*4*)**

A 35 μM solution of 5-HTPP $\cdot$ $2H_2O$ (2.69 mg) in 0.01 M HCl (300 ml) was electro-oxidized at pyrolytic graphite electrodes at 700 mV for 10 min. At this time, another 2.69 mg of 5-HTPP $\cdot$ $2H_2O$ was added to the solution in the working electrode compartment and the electrolysis continued for a further 10 min. This process was repeated a total of six times. Throughout the electrolysis the solution in the working electrode compartment was bubbled vigorously with N_2 gas and stirred with a Teflon-coated magnetic stirring bar. The counter electrode compartment contained

0.01 M HCl solution. Aliquots (ca. 100 ml) of the bright purple product solution (λ_{max} 532, 350 nm) were introduced onto the preparative reversed-phase column directly through one HPLC pump and the components were separated using preparative HPLC method I. The solution eluted under the chromatographic peak corresponding to **4** at a retention time (t_R) of 16.5 min was collected. A freshly chromatographed solution of **4** in the mobile phase (pH 3.8 ammonium acetate solution containing ca. 4% MeCN) exhibited a characteristic purple color (λ_{max} 540, 354, 240 nm). Spectroscopic evidence for the structure of **4** has been presented in detail elsewhere (*18*). Relatively dilute solutions of **4** ($\leq$200 μM) in the chromatographic mobile phase were stable for a few hours at room temperature. However, at higher concentrations (ca. 1 mM) a dark purple precipitate appeared within a few minutes. In pH 7.4 phosphate buffer (μ = 1.0) even a very dilute solution of **4** (40 μM) partially decomposed within 10 min although the products formed remain to be identified.

Synthesis of 7-S-Glutathionyltryptophan-4,5-dione **(7)**

A freshly chromatographed (method I) solution of dione **4** (20 ml; ca. 0.8 mM), prepared as described above, was treated with solid GSH (GSH : **4** mole ratio 1.2 : 1). The resulting solution was then diluted to 30 ml by addition of chromatographic solvent A and the pH was adjusted from 3.8 to 6.5–7.0 by careful addition of concentrated NH_4OH. The pH was then adjusted to 1–2 with concentrated HCl solution. HPLC (method II) of the product solution showed that two components were present. The minor product (t_R = 15.1 min) was colorless in the HPLC mobile phase (λ_{max} at pH 3.8 318, 274, 218 nm). This spectrum was virtually identical to that of 7-*S*-glutathionyl-4,5-dihydroxytryptamine (*19*). Furthermore, in the presence of molecular oxygen this product turned purple and gave a spectrum and t_R value that were identical to those of **7.** Accordingly, this minor product was 7-*S*-glutathionyl-4,5-dihydroxytryptophan **(6).** The major product (t_R = 19.3 min) was collected, following repetitive 50-ml injections of the reaction solution, in a flask maintained at −80°C and then freeze-dried until ca. 70% of the solvent was removed. The remaining frozen brown residue was dissolved in 0.01 M HCl to give a concentration of **7** of ca. 0.5 mM, and the resulting solution was desalted using HPLC method VI. The eluent containing **7** was then diluted to a concentration of approximately 0.2 mM with deionized water and freeze-dried to give a brown fluffy solid.

Synthesis of 4-S-Glutathionyl-5-hydroxytryptophan **(5)**

5-HTPP · $2H_2O$ (5.12 mg, 0.5 mM) and GSH (30.7 mg, 2.5 mM) were dissolved in 40 ml of pH 7.4 phosphate buffer (μ = 0.1) and the resulting stirred solution was oxidized by controlled potential electrolysis at 300 mV for 1 h. During the course of the oxidation reaction the initially colorless solution turned a pale yellow color. After termination of the reaction, aliquots (10 ml) of the product solution were repetitively injected into the preparative HPLC system and components were separated using method VIII. Compound **5** eluted at t_R = 9.0 min. The solutions containing **5** were collected, combined, and freeze-dried. The resulting solid residue was then dissolved in 10 ml of deionized water and desalted using HPLC method

VI. The desalted solutions of **5** were collected at −80°C and freeze-dried to give a white solid.

Synthesis of 6,8-Bi-S-glutathionyl-α-amino-2-carboxy-10,11-dihydro-10,11-dioxo-11bH-indolo[2′3′ : 4,5]furo[3,2-h]pyrrolo[4,3,2-de]quinoline-11b-propanoic Acid **(*32*)** *and 6,8-Bi-S-glutathionyl-α-amino-10,11-dihydro-10,11-dioxo-11bH-indolo[2′,3′ : 4,5]furo[3,2-h]pyrrolo[4,3,2-de]quinoline-11b-propanoic Acid* **(*33*)**

A chromatographically pure solution of **7** (ca., 100 ml, 0.25 mM) dissolved in the mobile phase from HPLC method I (pH 3.8), prepared as described previously, was adjusted to pH 7.4 with 2 M NH_4OH. This solution, exposed to the atmosphere, was stirred for 8–12 h at room temperature. The entire solution was then pumped onto the preparative reversed-phase column and chromatographed using HPLC method I. The solution eluted under the single major peak (t_R = 37.5 min) which contained both **32** and **33** was collected at −80°C. This procedure was repeated several times. The combined solutions containing **32** and **33** were then freeze-dried. The resulting solid residue was dissolved in deionized water (ca. 10 ml) and **32** and **33** were separated using HPLC method IV. The eluents containing **32** (t_R = 24.9 min) and **33** (t_R = 29.2 min) were collected at −80°C and freeze-dried. The solid residues containing **32** and **33** were then individually dissolved in deionized water and desalted using HPLC method VI. The desalted solutions were then freeze-dried. Both **32** and **33** were obtained as orange-red solids.

Reactions between 7-S-Glutathionyltryptophan-4,5-dione and Free GSH

A vigorously stirred solution (100 ml) of **7** (ca. 0.25 mM) in the HPLC method I mobile phase (pH 3.8), prepared as described previously, was treated with GSH (46 mg, 1.5 mM). The resulting solution was then adjusted to pH 7.4 with 2 M NH_4OH. The initially bright purple color of **7** turned blue over the course of 4–5 h. The entire reaction solution was then introduced onto the preparative reversed-phase column and products were initially separated using HPLC method I. The solutions eluted under the chromatographic peaks corresponding to **14** (t_R = 17.1 min), **11** (t_R = 27.0 min), **23 + 27** (t_R = 32.0 min), and **20** (t_R = 33.1 min) were collected separately at −80°C. Following several repetitive experiments the combined solutions containing each of these products were freeze-dried. The solid sample containing both **23** and **27** (and ammonium acetate) was dissolved in deionized water (<10 ml) and injected onto the preparative reversed-phase column using HPLC method III. The solutions that eluted under peaks at t_R = 18.8 min (**27**) and 21.1 min (**23**) were collected and freeze-dried.

Compound **20** was also dissolved in the minimum volume of water (ca. 5 ml) and purified using HPLC method VI (t_R = 22.0 min). The solution containing **20** was then freeze-dried. The dry solid residue of **14** was dissolved in the minimum volume of deionized water and desalted using HPLC method V; the resulting solution was then freeze-dried to give a purple solid. Crude samples of **11, 20, 23,** and **27** were individually dissolved in deionized water and desalted using HPLC method VI. After freeze-drying, pure solid samples of **11** (red orange), **20** (brown), **23** (brown), and **27** (red-brown) were obtained.

Structure Elucidations

Structure elucidations for compounds **5, 7, 11, 14, 20, 23, 27, 32,** and **33** were based on UV–visible spectra, FAB–MS (including accurate mass measurements), and ^{1}H NMR spectra. Assignments of resonances in ^{1}H NMR spectra were always confirmed by homonuclear decoupling and two-dimensional correlated spectroscopy experiments. Where possible, ^{13}C NMR spectroscopy was also employed. However, several compounds (e.g., **7** and **14**) were too unstable to permit acquisition of ^{13}C NMR spectra; others (e.g., **23**) formed gels in the NMR tube.

4-S-Glutathionyl-5-hydroxytryptophan

This white solid dissolved in pH 7.4 phosphate buffer exhibited a UV spectrum with λ_{max}, nm (log ε_{max}, M^{-1} cm^{-1}) at 300 (3.92) and 214 (4.29). FAB–MS (thioglycerol/glycerol matrix) gave m/e = 526.1606 (MH^+, 58%, $C_{21}H_{28}N_5O_9S$; calcd. m/e = 526.1608). ^{1}H NMR (D_2O) gave δ 7.39 (d, J = 9.0 Hz, 1H, C(7) H), 7.26 (s, 1H, C(2) H), 6.87 (d, J = 8.7 Hz, 1H, C(6) H), 4.43 (dd, J = 8.1, 4.2 Hz, 1H, C(d) H), 4.32 (dd, J = 10.2, 5.1 Hz, C(α) H), 3.89 (dd, J = 15.0, 4.8 Hz, 1H C(b) H), 3.75 (t, J = 6.6 Hz, 1H, C(a) H), 3.71 (s, 2H, C(f) H_2), 3.30–3.16 (m, 3H, C(b′) H, C(e) H_2), 2.26 (dd, J = 15.6, 8.1 Hz, 1H, C(c) H), 2.16–1.95 (m, 3H, C(c′) H), C(β)-H_2). ^{13}C NMR (D_2O) gave δ 172.37, 171.11, 171.05, 170.91, 170.47 (5 carbonyl carbon resonances), 149.66, 130.18, 126.12, 125.78, 112.84, 109.79, 105.92, 104.27 (8 aromatic carbon resonances), 53.04, 52.37, 51.30, 39.19, 34.01, 28.98, 25.99, 23.68 (8 aliphatic carbon resonances).

7-S-Glutathionyltryptophan-4,5-dione

In pH 7.4 phosphate buffer **7** exhibited a UV–visible spectrum with λ_{max}, nm (log ε_{max}, M^{-1} cm^{-1}) at 544 (3.31), 370 sh (3.97), 3.42 (4.07), 244 (4.27). FAB–MS (glycerol/TFA matrix) gave m/e = 542.1578 ($MH_2 \cdot H^+$, 22%, $C_{21}H_{28}N_5O_{10}S$; calcd. m/e = 542.1557). ^{1}H NMR (D_2O) gave δ 6.83 (s, 1H, C(2) H), 5.83 (s, 1H, C(6) H), 4.12 (dd, J = 6.3, 7.8 Hz, 1H, C(α) H), 4.01 (s, 2H, C(f) H_2), 3.88 (t, J = 6.3 Hz, 1H, C(a) H), 3.50 (dd, J = 14.0, 5.7 Hz, 1H, C(e) H), 3.33 (dd, J = 13.8, 7.8 Hz, 1H, C(e) H), 3.24 (dd, J = 15.0, 4.8 Hz, 1H, C(β) H), 3.01 (dd, J = 14.7, 8.4 Hz, 1H, C(β') H), 2.56 (dd, J = 7.8, 5.7 Hz, 2H, C(c) H_2), 2.16 (dd, J = 14.1, 7.2 Hz, 2H, C(b) H_2). Addition of a drop of DCl caused a resonance at δ 4.66 (dd, J = 7.5, 6.0 Hz, 1H, C(d) H) to be resolved from the HOD peak. Compound **7** was insoluble in all nonexchanging deuterated solvents. The poor stability of **7** in D_2O precluded a ^{13}C NMR spectrum.

3,7-Bi-S-glutathionyltryptophan-4,5-dione ***(11)***

In pH 7.4 phosphate buffer **11** exhibited an UV–visible spectrum with λ_{max}, nm (log ε_{max}, M^{-1} cm^{-1}) at 502 (4.04), 382 (4.72), 260 sh (4.46), 232 sh (4.67). FAB–MS (thioglycerol/glycerol/TFA matrix) gave m/e = 845.2041 (MH^+, 2%, $C_{31}H_{41}N_8O_{16}S_2$; calcd. m/e = 845.2082). ^{1}H NMR (D_2O) gave δ 6.81 (s, 1H, C(2) H), 6.40 (s, 1H, C(6) H), 4.90 (dd, J = 9.0, 5.1 Hz, 1H, C(d) H), 4.66 (dd, J = 8.1, 5.7 Hz, 1H, C(d′) H), 4.13 (dd, J = 8.4, 4.8 Hz, 1H, C(α) H), 4.00 (s, 2H, C(f) H_2),

3.83 (s, 2H, C(f′) H_2), 3.81–3.76 (m, 2H, C(a) H, C(a′) H), 3.64 (dd, J = 14.1, 4.8 Hz, 1H, C(e) H), 3.54 (dd, J = 11.7, 4.2 Hz, 1H, C(e′) H), 3.47–3.39 (m, 2H, C(e) H, C(β) H), 3.27 (dd, J = 14.1, 8.1 Hz, 1H, C(e′) H), 3.06 (dd, J = 15.0, 8.4 Hz, 1H, C(β) H), 2.52 (dd, J = 16.8, 7.2 Hz, 4H, C(c) H_2, C(c′) H_2), 2.52 (dd, J = 14.4, 7.2 Hz, 4H, C(b) H_2, C(b′) H_2). ^{13}C NMR (D_2O) gave δ 172.62, 172.54, 171.18, 171.14, 170.97, 170.91, 170.83, 170.74, 170.61, 169.89, 149.56, 136.73, 123.09, 121.87, 121.23, 116.24, 114.83, 52.23, 51.31, 51.25, 50.85, 50.67, 42.46, 39.50, 39.42, 31.58, 29.38, 29.33, 25.30, 23.95, 23.90. These spectral data do not permit an unequivocal distinction between 3,7- and 3a,7-bi-*S*-glutathionyltryptophan-4,5-dione. However, subsequent discussion supports the proposed structure of **11.**

6,7-Bi-S-glutathionyltryptophan-4,5-dione ***(14)***

At pH 7.4 **14** exhibited a spectrum with λ_{max}, nm (log ε_{max}, M^{-1} cm^{-1}) at 528 (3.66), 344 sh (4.08), 310 (4.39), 240 (4.55), 214 (4.15). FAB–MS (3-nitrobenzyl alcohol matrix) gave m/e = 845.2096 (MH^+, 9%, $C_{31}H_{41}N_8O_{16}S_2$; calcd. m/e = 845.2082). ^{1}H NMR (D_2O) gave δ 6.91 (s, 1H, C(2) H), 4.71 (dd, J = 9.3, 4.5 Hz, 1H, C(d) H), 4.64 (dd, J = 9.3, 4.5 Hz, 1H, C(d′) H), 4.22 (dd, J = 7.8, 4.8 Hz, 1H, C(α) H), 4.06 (dd, J = 9.0, 4.5 Hz, 1H, C(a) H), 3.97 (s, 2H, C(f) H_2), 3.90 (s, 2H, C(f′) H_2), 3.90 (m, 1H, C(a′) H), 3.42 (dd, J = 14.7, 5.1 Hz, 1H, C(β) H), 3.23–3.08 (m, 3H, C(e) H, C(e′) H, C(β) H), 2.90 (dd, J = 14.4, 9.6 Hz, 2H, C(e′) H, C(e) H), 2.57–2.51 (m, 4H, C(c) H_2, C(c′) H_2), 2.42–2.32 (m, 1H, C(b) H), 2.21–2.13 (m, 3H, C(b) H, C(b′) H_2). ^{13}C NMR (D_2O) gave δ 178.22, 178.02, 174.48, 174.10, 174.00, 172.48, 172.40, 172.22, 172.03, 171.95, 171.80 (11 carbonyl carbon resonances), 149.57, 133.74, 125.04, 123.89, 118.49, 117.63 (6 aromatic carbon resonances), 54.65, 53.51, 52.60, 52.03, 51.96, 51.79, 40.69, 38.46, 38.00, 30.77, 30.52, 25.96, 25.62, 25.20 (14 aliphatic carbon resonances).

2,8-Bi-S-glutathionyl-1,6-dihydro-6-oxo-pyrrolo[4,3,2-de]quinoline-4-carboxylic Acid ***(20)***

At pH 7.4 a solution of **20** was blue with λ_{max}, nm (log ε_{max}, M^{-1} cm^{-1}) at 586 (3.92), 414 (3.92), 342 (4.07), 268 (4.37). However, in acidic solution **20** was orange-red with λ_{max}, nm (log ε_{max}, M^{-1} cm^{-1}) at 504 (3.75), 418 (3.89), 330 (3.97), 268 (4.35), 214 (4.50). FAB–MS (glycerol/TFA matrix) gave m/e = 825.1805 (MH^+, 8%, $C_{31}H_{37}N_8O_{15}S_2$; calcd. m/e = 825.1820). ^{1}H NMR (D_2O) gave δ 8.02 (s, 1H, C(3) H), 6.43 (s, 1H, C(7) H), 4.88 (dd, J = 8.4, 4.2 Hz, 1H, C(d) H), ca. 4.75 (C(d) H obscured by HOD in 1D experiments), 3.92 (s, 2H, C(f) H_2), 3.86–3.74 (m, 6H, C(f′) H_2, C(e) H, C(e′) H, C(a) H, C(a′) H), 3.60–3.49 (m, 2H, C(e) H, C(e′) H), 2.59–2.44 (m, 4H, C(c) H_2, C(c′) H_2), 2.17–2.06 (m, 4H, C(b) H_2, C(b′) H_2).

2,7,8-Tri-S-glutathionyl-1,6-dihydro-6-oxo-pyrrolo[4,3,2-de]quinoline-4-carboxylic Acid ***(23)***

A solution of **23** at pH 7.4 was blue and turned orange-red upon acidification. At pH 7.4 λ_{max}, nm (log ε_{max}, M^{-1} cm^{-1}) were 580 (3.52), 4.18 (3.36), 348 (3.85), 286 (3.95), 214 (4.21), and at pH 2.2, 486 (3.31), 424 (3.48), 322 (3.78), 276 (3.97),

212 (4.28). All attempts to obtain a mass spectrum (EI, FAB–MS) on **23** were unsuccessful. The very low solubility of this compound in all matrices employed for FAB–MS probably account for the inability to obtain a useful mass spectrum. The structure proposed for **23** thus was based on its ^{1}H NMR spectrum and a comparison of this and other spectral properties with those of **27.** ^{1}H NMR (D_2O; 50°C) gave δ 8.51 (s, 1H, C(3) H), 5.23 (dd, J = 8.4, 5.7 Hz, 1H, C(d) H), 5.16 (dd, J = 7.6, 5.4 Hz, 1H, C(d′) H), ca. 4.80 (C(d″) H; masked by HOD in 1D experiments), 4.73 (dd, J = 14.7, 6.6 Hz, 1H, C(e′) H), 4.25 (s, 2H, C(f) H_2), 4.22 (d, J = 2.7 Hz, 2H, C(f′) H_2), 4.27–4.20 (m, 2H, C(e) H, C(e′) H), 4.14–4.06 (m, 3H, C(a) H, C(a′) H, C(a″) H), 4.02 (s, 2H, C(f″) H_2), 3.91 (dd, J = 13.5, 8.1 Hz, 1H, C(e)H), 3.63 (dd, J = 14.1, 4.8 Hz, 1H, C(e″) H), 3.54 (dd, J = 14.1, 8.4 Hz, 1H, C(e″) H), 2.88–2.73 (m, 6H, C(c) H_2, C(c′) H_2, C(c″) H_2), 2.48–2.35 (m, 6H, C(b) H_2, C(b′) H_2, C(b″) H_2).

2,7,8-Tri-S-glutathionyl-1,6-dihydro-6-oxopyrrolo[4,3,2-de]quinoline **(*27*)**

At pH 7.4 solutions of **27** were blue. In acidic solution **27** gave an orange color. Representative spectra of **27,** λ_{max}, nm (log ε_{max}, M^{-1} cm^{-1}) were at pH 7.4, 580 (3.74), 414 (3.72), 334 (4.26), 272 (4.19), 222 (4.30), and at pH 2.2, 452 (3.58), 428 (3.59), 306 (4.09), 276 (4.09), 214 (4.27). FAB–MS (3-nitrobenzyl alcohol/glycerol/TFA matrix) gave m/e = 1086.2579 (MH^+, 4.5%, $C_{40}H_{52}N_{11}O_{19}S_3$; calcd. m/e = 1086.2603) in addition to ions at m/e = 1087 (4%), 1088 ($MH_2 \cdot H^+$, 5%). ^{1}H NMR (D_2O) gave δ 8.72 (d, J = 4.8 Hz, 1H, C(3) H), 7.74 (d, J = 4.8 Hz, 1H, C(4) H), 4.97 (dd, J = 7.8, 5.4 Hz, 1H, C(d) H), 4.85 (C(d′) H; obscured by HOD in 1D experiments), 4.48 (m, 2H, C(d″) H, C(e′) H), 3.97 (dd, 13.8, 5.1 Hz, 1H, C(e) H), 3.91 (s, 2H, C(f) H_2), 3.66 (s, 2H, C(f″) H_2), 3.91–3.66 (m, 4H, C(e′) H, C(a) H, C(a′) H, C(a″) H), 3.60 (dd, J = 14.1, 8.1 Hz, 1H, C(e′) H), 3.34 (dd, J = 14.4, 4.5 Hz, 1H, C(e″) H), 3.20 (dd, J = 14.1, 9.0 Hz, 1H, C(e″) H), 2.55–2.35 (m, 6H, C(c) H_2, C(c′) H_2, C(c″) H_2), 2.16–2.01 (m, 6H, C(b) H_2, C(b′) H_2, C(b″) H_2).

6,8-Bi-S-glutathionyl-α-amino-2-carboxy-10,11-dihydro-10,11-dioxo-11bH-indolo[2′,3′: 4,5]furo[3,2-h]pyrrolo[4,3,2-de]quinoline-11b-propanoic acid **(*32*)**

At pH 7.4, **32** exhibited a UV–visible spectrum with λ_{max}, nm (log ε_{max}, M^{-1} cm^{-1}) at 476 (4.36), 408 sh (4.14), 290 (4.37). Unlike compounds **20, 23,** and **27** the UV–visible spectrum of **32** did not change significantly in acidic solution. FAB–MS (thioglycerol/glycerol matrix) gave m/e = 1055 (MH^+, 2%). ^{1}H NMR (D_2O) gave δ 8.18 (s, 1H, C(3) H), 7.32 (s, 1H, C(4) H), 6.92 (s, 1H, C(9) H), 5.30 (d, J = 8.4 Hz, 1H, C(d′) H), 5.04 (dd, J = 9.0, 4.2 Hz, 1H, C(a′) H), 4.38 (t, J = 6.3 Hz, 1H, C(d) H), 4.09–4.03 (m, 2H, C(α) H, C(e′) H), 3.93 (s, 2H, C(f′) H_2), 3.70 (t, J = 6.3 Hz, 1H, C(a) H), 3.47 (d, J = 1.1 Hz, 2H, C(f) H_2), 3.43–3.23 (m, 4H, C(e′) H, C(e) H_2, C(β) H), 3.07 (t, J = 12.0 Hz, 1H, C(β) H), 2.64–1.98 (m, 8H, C(c) H_2, C(c′) H_2, C(b) H_2, C(b′) H_2).

6,8-Bi-S-glutathionyl-α-amino-10,11-dihydro-10,11-dioxo-11bH-indolo[2′,3′: 4,5]furo[3.2-h]pyrrolo[4,3,2-de]quinoline-11b-propanoic Acid

At pH 7.4 the UV–visible spectrum of **33** exhibited λ_{max}, nm (log ε_{max}, M^{-1} cm^{-1}) at 460 (4.35), 406 sh (4.19), 294 sh (4.29), 278 (4.38). FAB–MS (thioglycerol/glycerol/H_2O matrix) gave m/e = 1010 (M^+, 2%), 1011 (MH^+, 2%), 1012 ($MH \cdot H^+$, 1.5%), 1013 ($MH_2 \cdot H^+$, 1%). ^1H NMR (D_2O) gave δ 8.60 (d, J = 5.1 Hz, 1H, C(3) H), 7.61 (d, J = 4.8 Hz, 1H, C(2) H), 7.33 (s, 1H, C(4) H), 7.06 (s, 1H, C(9) H), 5.10–5.04 (m, 2H, C(d′) H, C(a′) H), 4.31 (t, J = 6.0 Hz, 1H, C(d) H), 3.95 (t, J = 6.3 Hz, 1H, C(α) H), 3.90 (m, 3H, C(f′) H_2, C(e) H), 3.70 (t, J = 6.3 Hz, 1H, C(a) H), 3.38 (d, J = 4.8 Hz, 2H, C(f) H_2), 3.31–3.20 (m, 5H, C(e′) H, C(e) H_2, C(β) H_2), 2.65–2.38 (m, 4H, C(c′) H_2, C(c) H_2), 2.19–1.99 (m, 4H, C(b′) H_2, C(b) H_2). ^{13}C NMR (D_2O) gave δ 174.06, 173.72, 172.54, 172.35, 172.28, 171.90, 170.68, 170.55, 169.66, 166.79, 162.05, 150.77, 150.59, 143.20, 136.35, 133.09, 132.91, 127.31, 123.67, 123.54, 123.47, 121.63, 116.22, 113.80, 109.29, 108.07, 86.02, 56.27, 54.06, 53.89, 51.95, 51.36, 39.99, 39.53, 33.14, 29.63, 29.58, 29.22, 27.73, 26.77, 24.12.

RESULTS

Electrochemical oxidation of 5-HTPP in the Presence of GSH

A cyclic voltammogram of 5-HTPP (200 μM) in pH 7.4 phosphate buffer (μ = 1.0) at a sweep rate (ν) of 1 V s^{-1} is shown in Fig. 1A. Peak I_a (E_p = 332 mV) corresponds to the 2e, H^+ oxidation of 5-HTPP to a cationic intermediate represented by resonance structures **1a/1b** in Scheme I (*10*). After scan reversal at $\nu \geq$ 1 V s^{-1} peak I_c (E_p = 296 mV) corresponding to the reduction of **1** to 5-HTPP appears. Peak II_c (E_p = −210 mV) corresponds to the reduction (2e, $2H^+$) of **4** to 4,5-dihydroxytryptophan (**3**) and peak II_a (E_p = −200 mV) to the reverse reaction. Diol **3,** formed by nucleophilic addition of water to putative intermediate **1,** is immediately oxidized to dione **4** at peak I_a potentials and, hence, peaks II_c and II_a appear after having initially scanned through oxidation peak I_a. At sufficiently fast sweep rates (ν > 10 V s^{-1}) the peak current (i_p) for reduction peak I_c becomes equal to that of peak I_a and, correspondingly, the peak II_c/peak II_a couple disappears. A cyclic voltammogram (ν = 1 V s^{-1}) of 5-HTPP (200 μM) in the presence of GSH (2.0 mM) is presented in Fig. 1B which reveals that the tripeptide has no significant effect on E_p or i_p for oxidation peak I_a although i_p for reduction I_c was decreased somewhat. Similarly, in the presence of GSH the i_p values for the peak II_c/peak II_a couple decrease somewhat although even in the presence of very large (e.g., 50-fold) molar excesses of the tripeptide this couple remained a significant feature of cyclic voltammograms of 5-HTPP. GSH exhibited no voltammetric peaks at the PGE over the potential range employed in Fig. 1.

At a very slow sweep rate (ν = 5 mV s^{-1}) E_p for oxidation peak I_a of 5-HTPP (200 μM) in pH 7.4 phosphate buffer was 253 mV. In the presence of 2.0 mM GSH, E_p for peak I_a under the same experimental conditions was 264 mV. Accordingly, controlled potential electro-oxidation reactions were normally carried out for only a short period of time (10 min) at an applied potential of 200 mV in order to

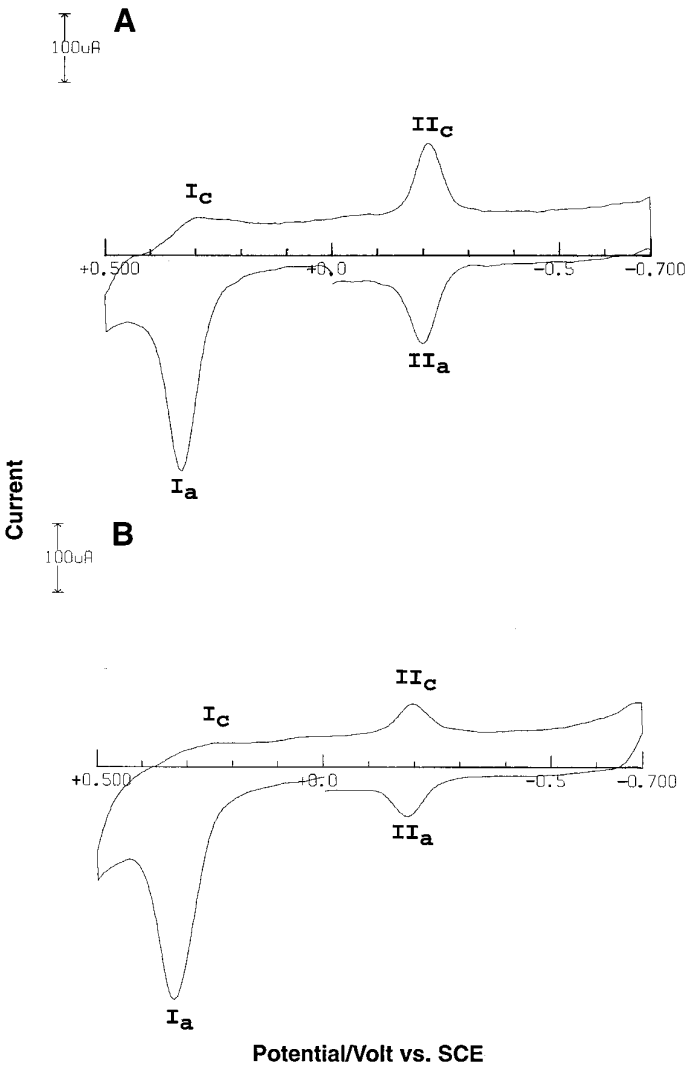

FIG. 1. Cyclic voltammograms at the PGE of (A) 200 μM 5-HTPP and (B) 200 μM 5-HTPP plus 2.0 mM GSH in pH 7.4 phosphate buffer (μ = 1.0). Sweep rate 1 V s^{-1}.

minimize secondary reactions. An HPLC chromatogram (method II) of the product solution formed following controlled potential electro-oxidation of 5-HTPP (0.5 mM) in pH 7.4 phosphate buffer under these conditions is shown in Fig. 2A. The major products of this reaction are diastereomers of 5,5′-dihydroxy-4,4′-bitryptophan **(2),** identified on the basis of their chromatographic t_R values and UV spectra compared to the authentic compounds (*10*). These dimers are formed as a result of nucleophilic addition of 5-HTPP to **1** (Scheme I). A third product was purple